Removal of contaminants of emerging concern from multicomponent systems using carbon dioxide activated biochar from lignocellulosic feedstocks

Bioresource Technology 340 (2021) 125561

Contents lists available at ScienceDirect

Bioresource Technology

journal homepage: www.elsevier.com/locate/biortech

Removal of contaminants of emerging concern from multicomponent systems using carbon dioxide activated biochar from lignocellulosic feedstocks

Ivan Kozyatnyk [a,1], Pierre Oesterle [a], Christian Wurzer [b], Ondřej Mašek [b], Stina Jansson [a,*]

[a] Department of Chemistry, Umeå University, SE-901 87 Umeå, Sweden
[b] UK Biochar Research Centre, School of GeoSciences, University of Edinburgh, EH9 3FF Edinburgh, UK

HIGHLIGHTS

- Adsorption from multicomponent CEC solution by three activated biochars was studied.
- Biochar porosity and CEC hydrophobicity both influenced the removal efficiency.
- Predominantly microporous peach stone biochar showed the lowest overall capacity.
- Hydrophilic CECs adsorbed best on ash-rich activated wheat straw biochars.
- Adsorption of hydrophobic CECs was highest on activated softwood biochar.

GRAPHICAL ABSTRACT

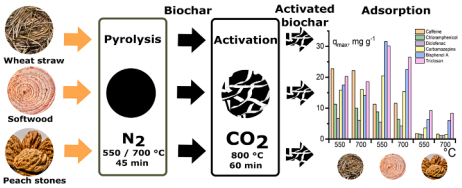

ARTICLE INFO

Keywords:
Activated carbon
Contaminants of emerging concern
Organic pollutants
Emerging contaminants
Wastewater remediation

ABSTRACT

Adsorption of six contaminants of emerging concern (CECs) – caffeine, chloramphenicol, carbamazepine, bisphenol A, diclofenac, and triclosan – from a multicomponent solution was studied using activated biochars obtained from three lignocellulosic feedstocks: wheat straw, softwood, and peach stones. Structural parameters related to the porosity and ash content of activated biochar and the hydrophobic properties of the CECs were found to influence the adsorption efficiency. For straw and softwood biochar, activation resulted in a more developed mesoporosity, whereas activation of peach stone biochar increased only the microporosity. The most hydrophilic CECs studied, caffeine and chloramphenicol, displayed the highest adsorption (22.8 and 11.3 mg g^{-1}) onto activated wheat straw biochar which had the highest ash content of the studied adsorbents (20 wt%). Adsorption of bisphenol A and triclosan, both relatively hydrophobic substances, was highest (31.6 and 30.2 mg g^{-1}) onto activated biochar from softwood, which displayed a well-developed mesoporosity and low ash content.

1. Introduction

Contaminants of emerging concern (CECs) are characterised by their ubiquity, persistence, and potential for, or established, risk to human health and the environment (Galindo-Miranda et al., 2019). The CECs observed in this study represent several different classes of compounds.

* Corresponding author.
E-mail address: stina.jansson@umu.se (S. Jansson).
[1] Current affiliation: Department of Health, Medicine and Caring sciences, Unit of Clinical Medicine, Occupational and Environmental Medicine, Linköping University, 581 83 Linköping, Sweden.

https://doi.org/10.1016/j.biortech.2021.125561
Received 2 June 2021; Received in revised form 8 July 2021; Accepted 10 July 2021
Available online 19 July 2021

Chloramphenicol (an antibiotic), carbamazepine (an anticonvulsant) and diclofenac (a non-steroidal anti-inflammatory drug, or NSAID) represent commonly used pharmaceuticals (Patel et al., 2019). Bisphenol A is a chemical widely used in plastic production (Suzuki et al., 2004), whereas caffeine is a commonly consumed stimulant (Buerge et al., 2003) and triclosan is an antimicrobial disinfectant used in personal care products (Ebele et al., 2017). All these compounds are frequently found in water sources (surface, subsurface and ground waters) influenced by human activity and may adversely affect aquatic life and human health (Patel et al., 2019).

Recent scientific research focuses on strategies for reducing CECs in wastewater effluents based on conventional and advanced treatment processes (Rizzo et al., 2019). One of the most commonly used methods for removing CECs from water is adsorption onto activated carbon (AC) (Mailler et al., 2016). ACs have many structural and morphological features that give them excellent adsorbent properties, such as a large specific surface area, high porosity, and reactive surface chemistry (Tan et al., 2017).

However, AC production is costly, with the current price of 200 mesh AC powder ranging from 800 to 5000 United States dollars (USD) per tonne (Yunus et al., 2020). Furthermore, the most significant contributor to a negative environmental impact in AC production is the use of non-renewable feedstocks, including fossil coal. The activation process has a high energy demand (Bayer et al., 2005) and uses hazardous chemicals like potassium hydroxide (KOH) and phosphoric acid (H_3PO_4) (Sepúlveda-Cervantes et al., 2018). Physical activation usually occurs at temperatures between 800 °C and > 1000 °C in the presence of oxidizing gas compounds such as carbon dioxide or steam (Dalai & Azargohar, 2007). Despite physical activation requiring high process temperatures and yielding lower carbon amounts than chemical activation, it has the advantage of avoiding the use of toxic and environmentally-damaging activation agents (Sajjadi et al., 2019) and could potentially use CO_2 produced from other industries.

Several alternative low-cost carbon adsorbents based on renewable organic residues from agriculture and industry have been examined as possible replacements for fossil-based AC for water treatment (Thompson et al., 2016). Biochar is a stable carbon material obtained by pyrolysis, i.e. thermochemical conversion, of biomass in an oxygen-lean or oxygen-free atmosphere (Wang et al., 2020). Biochar reportedly adsorbs organic and inorganic pollutants (Tan et al., 2015). However, biochar typically has low porosity ranging from < 100 $m^2\ g^{-1}$ (Sajjadi et al., 2019) up to 460 $m^2\ g^{-1}$ (Park et al., 2013), contrary to typical AC surface areas ranging between 500 and 1500 $m^2\ g^{-1}$, or even as high as 3000 $m^2\ g^{-1}$ (Bernal et al., 2018). Therefore, the adsorption capacity and selectivity of biochar are relatively low compared to other porous carbon materials (Ahmed et al., 2016).

However, the use of materials with higher adsorption capacities proved an efficient means of reducing the overall environmental impacts of carbonaceous adsorbents (Kozyatnyk et al., 2020; Thompson et al., 2016). Biochar activation using chemical and physical (Dalai & Azargohar, 2007) methods can greatly enhance its specific surface area and pore volume and, thus, potentially the biochar adsorption capacity (Tan et al., 2017). Moreover, the use of locally or regionally available low-cost renewable feedstocks would likely be more advantageous from an economic and environmental perspective than conventional fossil-based adsorbents (Mohan et al., 2014).

The physical and chemical properties of biochar depend on its source feedstock and processing conditions (Zhao et al., 2013), which are partly explained by the decomposition behaviour of the main biomass components (cellulose, hemicellulose and lignin) during pyrolysis. Pyrolysis of hemicellulose and cellulose occurs quickly during the initial pyrolysis stages, with peak hemicellulose weight loss at 220 °C – 315 °C followed by cellulose degradation at 315 °C – 400 °C (Yang et al., 2007). Lignin, on the other hand, is more stable during pyrolysis, with weight loss occurring over a wide temperature range (from 160 °C to 900 °C) (Yang et al., 2007). Feedstock composition may also influence the chemical composition and morphology of activated biochar (Park et al., 2013; Rodriguez Correa et al., 2017; Tan et al., 2017; Zhao et al., 2013).

This work aimed to study the influence of certain properties of CO_2-activated biochar from three different lignocellulosic feedstocks on the removal of six CECs in multicomponent water. The activated biochar properties investigated were specific surface area, porosity, elemental composition, and proximate analysis, and the six CECs in the multicomponent water were chloramphenicol, carbamazepine, diclofenac, bisphenol A, caffeine, and triclosan. Understanding the performance of activated biochar as adsorbents for removal of priority CECs and any associations with the source feedstock composition and biochar production conditions would allow further improvement of biochar sorption capacity and specificity.

2. Materials and methods

2.1. Feedstock selection and biochar preparation and activation

The feedstocks selected for biochar preparation represent biomass assortments containing differing amounts of hexosans (mainly representing cellulose), pentosanes (mainly representing hemicellulose), and lignin (Table 1). Feedstock compositions were analysed for inherent amounts of lignin (Klason and acid soluble), lignocellulosic sugars (hexosans and pentosans), ash, and extractives by an external laboratory (Celignis Analytical, Limerick, Ireland). Softwood has high cellulose content (>45%), high total sugar content (59.5%) comprised mainly of hexosans (53.1% in whole biomass), and a lignin content of 26.9%. In contrast, peach stone biomass had high lignin content (44.8%) and limited total sugar contents (15.8% hexosans and 19.3% pentosans). The third feedstock, wheat straw, had the lowest lignin content (17.2%) and a total sugar content (58.4%) comparable to that of softwood but with a greater amount of pentosanes (22.2%). Moreover, wheat straw contained higher amounts of extractives (9.7%) and ash (6.3%) than the other two feedstocks (6.3–6.9% of extractives and < 1% of ash).

The wheat straw and softwood biochar were selected from the standard biochars produced at the UK Biochar Research Centre (UKBRC). These biochar materials were produced using a pilot-scale rotary kiln pyrolysis unit at 550 °C and 700 °C, respectively, at a heating rate of approximately 85 °C min^{-1} and residence time at the highest treatment temperature (HTT) of approximately 5 min. The unit comprised a variable speed screw-feeder with an attached hopper, a sealed rotating drum (inner diameter 0.244 m, heated length 2.8 m) heated by a set of electric heaters arranged in three heater banks of 16.67 kW each, a char handling screw conveyor, a collection vessel, and an afterburner chamber (Mašek et al., 2018).

Fruit stones (189 g) were collected from peaches purchased from a local grocery store in Umeå, Sweden. The peach stones were crushed to a particle size < 1 cm and dried at 110 °C to a constant weight (140 g). The lignocellulosic composition of the peach stones feedstock (Table 1) fell within the range of compositional data reported in previous studies (Blasi et al., 2019; Li et al., 2018b). Approximately 50 g of crushed peach stones were placed in a batch pyrolysis unit with a vertical quartz tube (inner diameter 50 mm) at a sample bed depth of around 200 mm and heated using a 12-kW infrared gold image furnace (P610C; ULVAC-RIKO, Yokohama, Japan, see (Mašek et al., 2018). Before pyrolysis, the reactor was purged with nitrogen to eliminate any residual oxygen within the system. The peach stones were pyrolyzed at a heating rate of 15 °C min^{-1}, with HTTs of 550 °C and 700 °C and a residence time of 45 min at HTT. After pyrolysis, the system was cooled under nitrogen flow to prevent biochar oxidation. As previously shown (Mašek et al., 2018), no statistically significant differences were observed among the characteristics of the UKBRC standard biochar produced using pilot-scale pyrolysis units and those produced in lab-scale pyrolysis units.

Biochar activation was conducted in the abovementioned batch pyrolysis unit using carbon dioxide as the activation agent. Prior to activation, biochar materials were crushed to a particle size < 2 mm.

Table 1
Composition of feedstocks (in % dry weight).

Feedstock	Total sugars	Hexosans	Pentosans	Klason lignin	Acid soluble lignin	Extractives	Ash
Wheat straw	58.4	36.2	22.2	17.2	1.8	9.7	6.3
Softwood	59.5	53.1	6.4	26.9	0.5	6.3	0.3
Peach stones	35.1	15.8	19.3	44.8	1.2	6.9	0.6

Approximately 30 g of each biochar were heated to 800 °C under continuous CO_2 flow at a rate of 1.2 L min^{-1}, with a heating rate of 30 °C min^{-1} and residence time at the HTT of 60 min. After activation, the biochar was allowed to reach room temperature within the reactor under continued CO_2 flow. The biochar and activated biochar were then crushed using a pestle and mortar and sieved to obtain a particle size between 0.50 and 0.125 mm. The samples were washed with 0.1 mol L^{-1} hydrochloric acid (HCl) to remove the inorganic phase, and rinsed with deionised water until the pH stabilised. Each biochar was labelled according to its source feedstock type (wheat straw pellets (WSP), softwood pellets (SWP) and peach stones (PS)), the HTT for pyrolysis (550 and 700), and whether it was activated (an (A) denoting activation).

2.2. Biochar characterization

Proximate analysis was conducted using thermogravimetric analysis with differential scanning calorimetry (TGA/DSC-1; Mettler-Toledo, UK). Approximately 10 mg of sample was placed in an alumina crucible and heated to 110 °C under nitrogen flow for 10 min to determine moisture content. The sample was further heated to 900 °C at 25 °C min^{-1} and held for 10 min to determine volatile matter content, followed by 30 min combustion in air at 900 °C to determine ash content, assuming complete combustion of organic matter. Fixed carbon content was calculated by subtracting moisture, volatile matter and ash content from the initial weight of the sample. All analyses were performed in triplicate.

Elemental bulk composition analysis (i.e., of carbon (C), hydrogen (H), nitrogen (N), and oxygen (O)) was performed in triplicate using a Flash Smart Elemental Analyzer (Thermo Fisher Scientific, USA). Samples were ball milled and dried at 105 °C overnight. Approximately 1.5 mg of the dried sample was weighed out with an accuracy of 0.001 mg, double wrapped into tin capsules and stored in a desiccator. Before analysis, the samples were placed in a helium (He)-flushed autosampler carousel to avoid moisture uptake. C, H and N were measured by flash combustion at 950 °C and O was calculated by difference.

The pH and electrical conductivity of each biochar were determined before and after activation using 0.5 g of biochar and 10 mL of deionised water, with a shaking time of 1.5 h (see (Singh et al., 2017) for more details).

The TriStar 3000 automated nitrogen sorption/desorption instrument (Micromeritics, Norcross, GA, USA) was used to analyse the porosity properties of the biochar. A 0.1 g mass of dried biochar was degassed under nitrogen flow at 120 °C for 2 h. (see (Mustafa et al., 2021) for more details).

2.3. Adsorption of CECs

The selection of CECs for adsorption experiments was based on environmental relevance (occurrence in aquatic environments and potential environmental impact), as well as octanol–water partition coefficient (K_{ow}) which reflects the hydrophilic-hydrophobic properties of a substance (Delle Site, 2001; Li et al., 2018a). Typically, compounds with a $K_{ow} > 2$ and water solubilities < 100 mg L^{-1} are considered hydrophobic (Elzerman & Coates, 1987). The six CECs selected for this study have K_{ow} values ranging between −0.07 to 4.76 as follows: caffeine, −0.07; chloramphenicol, 1.02; carbamazepine, 2.67; bisphenol A, 3.43; diclofenac, 4.06; and triclosan, 4.76 (https://pubchem.ncbi.nlm.nih.gov/compound) (see additional properties of the CECs in Appendix, Table A1). The multicomponent CEC stock solution was prepared in methanol with each CEC at a concentration of 5 g L^{-1}, except for triclosan which had a 3 g L^{-1} concentration due to its low water solubility.

The adsorption experiments were conducted at ambient temperature (20 °C) in enclosed tubes containing 50 mg of activated biochar and 50 mL of CEC solution. The CEC solution (concentration 100 mg L^{-1} in ultrapure water for all CECs except triclosan at 60 mg L^{-1}) was further diluted to the following concentrations: 5, 7, 10, 12, 15, 20, 30, 40, 80 and 100 mg L^{-1} for caffeine, chloramphenicol, carbamazepine, bisphenol A, and diclofenac; and 3, 4.2, 6, 7.2, 9, 12, 18, 24, 48 and 60 mg L^{-1} for triclosan. Preliminary tests of CEC adsorption onto commercial AC Norit GSX (Alfa Aesar, Germany) were performed to confirm that the selected concentration ranges were sufficient for studying the initial steep part of the adsorption isotherm at lower CEC concentrations as well as the flatter part of the isotherm at higher CEC concentrations when the adsorbent is at or close to saturation (see Table 2 and Appendix, Figure A1). The pH of the CEC solutions was neutralised using 1 mol L^{-1} sodium hydroxide (NaOH). The tubes were shaken with an orbital shaker at 50 rpm for 24 h, after which the CEC solution was filtered off using 0.45–μm nitrocellulose membrane syringe filters.

CEC concentrations were determined using a HP 1100 Chromatography System (Agilent, Germany) and a Hypersil octadecylsilane (ODS) 5 μm C18, 100 × 2.1 mm column. The column temperature was kept constant at 30 °C. The analyses were performed using acetonitrile and 0.1 mol L^{-1} ammonium acetate buffer at a flow rate of 0.5 mL min^{-1}. The injection volume was 10 μL and CECs were detected using UV-absorption measurements at 254 nm for caffeine, chloramphenicol, carbamazepine and diclofenac and at 280 nm for triclosan. Bisphenol A was detected using a fluorescence detector at an excitation wavelength of 280 nm and emission wavelength of 340 nm.

The equilibrium adsorption (q_{eq}) was calculated as follows:

$$q_{eq} = \frac{(C_0 - C_{eq}) \bullet V}{m} \quad (1)$$

where C_0 (initial) and C_{eq} (equilibrium) denote CEC concentrations (mg L^{-1}), V is the solution volume (L), and m is the mass of sorbent (g).

The maximum adsorption (q_{max} (mg g^{-1})) was calculated from the linear form of the Langmuir model of adsorption (Langmuir, 1918):

$$\frac{1}{q_{eq}} = \frac{1}{q_{max}} + \frac{1}{q_{max} K_L C_{eq}} \quad (2)$$

where K_L denotes the Langmuir isotherm constant (L mg^{-1}). The values of q_{max} and K_L were calculated from the intercept and slope of the Langmuir plot of $1/C_{eq}$ versus $1/q_{eq}$.

Assessment of adsorption performance of the activated biochar was also performed using the Freundlich model of adsorption (Freundlich, 1907).

$$q_{eq} = K_F C_{eq}^{1/n} \quad (3)$$

where K_F and n are the Freundlich constants for a given adsorbate and adsorbent, respectively, at a specific temperature.

3. Results and discussion

3.1. Physiochemical characterization of the biochar

Differences in pyrolysis temperature and feedstock (Yang et al.,

Table 2
Properties of non-activated and CO_2-activated biochar.

Sample*	Pyrolysis temperature, °C	Yield, % dry weight (dw) from feedstock	C, wt%	H, wt %	N, wt %	O, wt%	H/C	O/C	Total ash, wt%	pH	Electrical conductivity, dS/m	Volatile matter, % dw	Fixed carbon, % dw	Specific surface area, m^2 g^{-1}	Micropore surface area, m^2 g^{-1}	External surface area, m^2 g^{-1}	Total pore volume, cm^3 g^{-1}	Micropore volume, cm^3 g^{-1}	Average pore width, nm
WSP550	550	24.1	68.9	2.8	-**	8.8	0.48	0.10	19.5	10.3	1.49	18.4	62.2	15.9	7.8	8.1	0.02	0.00	4.87
WSP700	700	23.5	70.6	2.1	0.5	9.2	0.35	0.10	17.7	10.1	2.40	15.5	66.8	59.5	46.9	12.6	0.04	0.02	2.87
WSP550A	550	16.5	68.3	0.7	1.1	7.3	0.12	0.08	22.6	10.1	0.45	8.9	68.6	493.3	400.1	93.2	0.28	0.20	2.28
WSP700A	700	18.2	71.6	0.7	1.0	6.9	0.12	0.07	19.8	10.4	0.75	8.8	71.4	451.8	362.2	89.5	0.26	0.19	2.32
SWP550	550	21.8	82.8	3.3	-**	11.8	0.48	0.11	2.0	8.4	0.07	18.7	79.3	3.4	2.0	1.4	0.00	0.00	3.81
SWP700	700	17.3	89.5	2.5	-**	5.4	0.33	0.05	2.6	9.1	0.21	12.4	85.0	204.6	176.5	28.1	0.12	0.09	2.29
SWP550A	550	15.2	93.3	0.9	-**	4.3	0.11	0.03	1.5	7.4	0.25	7.3	91.3	530.3	365.9	164.4	0.31	0.19	2.34
SWP700A	700	13.5	92.0	0.9	-**	5.5	0.12	0.04	1.6	8.0	0.29	7.9	90.7	484.5	332.5	152.2	0.28	0.17	2.35
PS550	550	32.3	86.9	2.5	-**	9.4	0.34	0.08	1.2	9.0	0.08	14.4	84.4	315.7	257.6	58.1	0.17	0.13	2.14
PS700	700	28.8	87.4	1.3	-**	10.8	0.18	0.09	0.5	8.2	0.05	9.0	90.5	309.1	274.2	34.9	0.16	0.14	2.11
PS550A	550	27.3	93.0	0.8	-**	5.5	0.10	0.04	0.7	8.1	0.28	7.1	92.6	457.7	390.5	67.2	0.25	0.20	2.14
PS700A	700	26.8	92.3	0.9	-**	6.2	0.12	0.05	0.6	10.1	0.25	6.9	92.5	400.3	351.9	48.4	0.21	0.18	2.11

* WSP – wheat straw pellets biochar; SWP – softwood pellets biochar; PS – peach stones. 550 and 700 – pyrolysis temperatures (°C). A – activated biochar.
** - below detection limit.

2007) were reflected in the differences in biochar yield between the feedstocks studied (Table 2). Peach stones yielded more biochar, after pyrolysis (28.8 – 32.3%) and after activation (26.8 – 27.3%), than wheat straw and softwood (17.3 – 24.1% after pyrolysis and 13.5 – 18.2% after activation).

No covariations between activated biochar yield and pyrolysis temperature were observed; thus, biochar produced at the lower pyrolysis temperature as a precursor for activation was not expected to generate a higher overall yield. Biochar produced at 550 °C showed greater weight loss during activation than biochar produced at 700 °C (16.4–18.7% versus 7.9–15.5%), likely due to more volatile matter content in biochar generated at the lower temperature. This observation indicates incomplete carbonization during pyrolysis, possibly leading to a less aromatic carbon skeleton that would be prone to volatility during activation (Cagnon et al., 2009).

The notion of a less aromatic carbon skeleton is supported by the observation that the atomic H/C ratios for all biochar materials decreased from a range of 0.5–0.3 to around 0.1 during activation, indicating preferential loss of hydrogen over carbon and formation of more condensed aromatic structures (Schimmelpfennig & Glaser, 2012). The O/C ratio decreased for all biochar materials, with similar levels (0.08–0.03) for all activated biochar due to decarboxylation (Suliman et al., 2016). This observation suggests that activation produces more condensed aromatic (lower H/C ratio) and more carbonised (lower O/C ratio) structures (Schimmelpfennig & Glaser, 2012). The observation was further supported by the fixed carbon content which was highest for peach stone biochar (84.4–90.5% compared to 62.2–85.0% for the other biochar materials) and was about 4% higher for all feedstocks pyrolyzed at 700 °C compared to biochar obtained at 550 °C. Activation further increased the fixed carbon content to over 90% for peach stone and softwood biochar.

Ash content was 0.5–1.2% for peach stone biochar, 2.0–2.6% for softwood biochar, and 17.6–19.5% for wheat straw biochar. Ash content was feedstock dependent and increased with increasing pyrolysis temperature. Ash content in activated biochar was less than might be expected after activation due to the HCl wash for removing inorganic matter before adsorption experiments; for instance 19.8–22.6% in HCl-washed biochar compared to 27.5–28.1% for unwashed activated wheat straw biochar.

Biochar activation generated a more developed porosity (Table 2). Improved surface properties (i.e., specific surface area and pore volume) are known to enhance adsorption of organic matter onto carbonaceous materials (Zhu et al., 2018); this phenomenon was also observed in this study. The specific surface area exceeded 400 m^2 g^{-1} for all activated biochar compared to 3.4–316 m^2 g^{-1} for pristine biochar.

Nitrogen adsorption–desorption isotherms (see Appendix, Figure A2) were assigned as a composite of types I and II with a hysteresis loop of H4, according to International Union of Pure and Applied Chemistry (IUPAC) classification, which is often found for micro-mesoporous carbon materials (Thommes et al., 2015). A sharp step-down of the desorption branch of the isotherms for WSP-A and SWP-A biochar indicates the presence of mesopores (Thommes et al., 2015). From the pore size distribution (Fig. 1), one can conclude that pyrolysis of the straw and softwood feedstocks failed to produce well-developed porosity, except for softwood pyrolyzed at 700 °C which, together with peach stones (at both pyrolysis temperatures), mainly displayed micropore formation. Increasing the pyrolysis temperature from 550 °C to 700 °C increased the surface area and pore volume for both softwood and straw biochar; this effect was not observed for peach stones.

After activation, the pore size distribution curves of activated biochar originating from the same feedstocks were closely positioned (Fig. 1), irrespective of pyrolysis temperature. The specific surface areas, on the other hand, were approximately 50 m^2 g^{-1} greater for all 700A biochar materials than for the corresponding 550A biochar (Table 2). Activation of the softwood and straw biochar notably increased the specific surface area and pore volume of the materials with as much as a

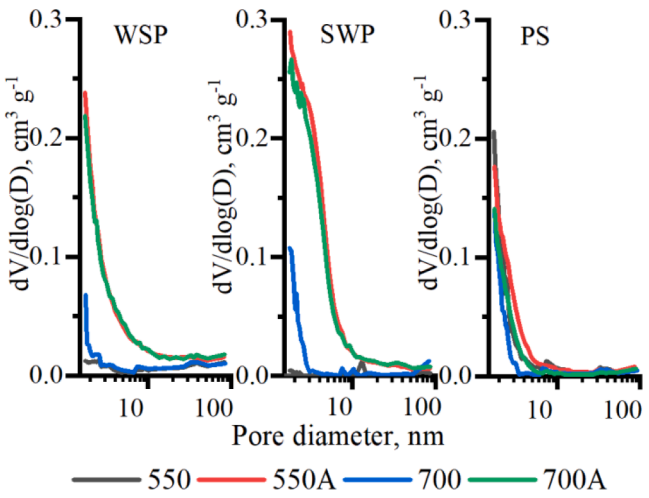

Fig. 1. Pore size distribution of biochar from N_2 adsorption isotherms using the BJH method. WSP – wheat straw; SWP – softwood; PS – peach stones. 550 and 700 – pyrolysis temperature (°C) of feedstocks. A – activated biochar.

two-fold increase for some, mainly because of micro- and mesopore formation. This is shown by the pore size distribution in Fig. 1 and the hysteresis shape (see Appendix, Figure A2). Mesopore (>2 nm) formation is important for adsorption applications of carbon materials since mesopores are crucial for their ability to adsorb organic substances (Yao et al., 2020). Although no substantial mesopore formation was observed after activation of the peach stone biochar, the pore volume increased from 0.16 – 0.17 to 0.21–0.25 $cm^3\ g^{-1}$, corresponding to an increase in surface area from about 300 $m^2\ g^{-1}$ to 400–450 $m^2\ g^{-1}$.

3.2. Adsorption properties of the activated biochar

The obtained adsorption isotherms of CECs (Fig. 2) showed L-behaviour according to Giles' classification (Giles et al., 1960), which is characteristic of monomolecular layer adsorption of CECs onto the surfaces of the activated biochar. L-type adsorption isotherms also indicate that there was no major competition between CEC molecules and water molecules for active adsorption centres on the carbon surface (Abdel daiem et al., 2015). L-type isotherms can become H-type when the adsorbate has high affinity for the adsorbent surface. H-type

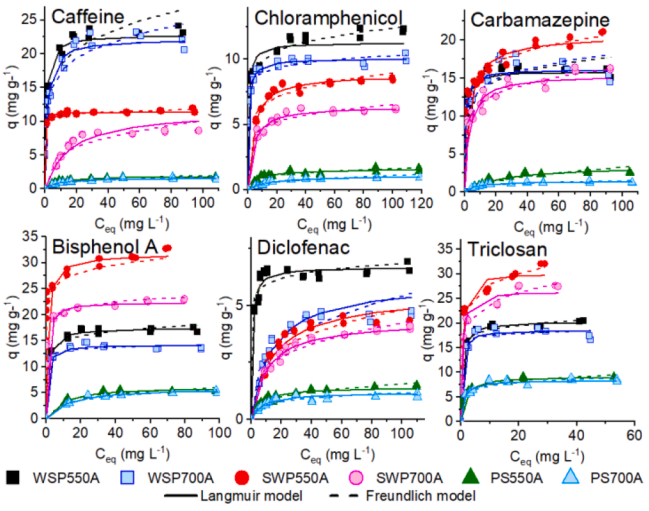

Fig. 2. Adsorption isotherms for caffeine, chloramphenicol, carbamazepine, bisphenol A, diclofenac, and triclosan on activated biochar from wheat straw (WSP550A and WSP700A), softwood (SWP550A and SWP700A), and peach stones (PS550A and PS700A).

isotherms differ from L-type by a complete adsorption at low CEC concentrations that decreases at an approximate equilibrium concentration, then tends to decrease more slowly at higher concentrations. H-type isotherms were observed for adsorption of chloramphenicol, carbamazepine, bisphenol A and triclosan onto SWP and WSP activated biochar, and for caffeine onto SWP500A, diclofenac onto WSP500A, and triclosan onto PS500A and PS700A.

Based on R^2 values (Table 3), the Langmuir adsorption model, in most cases, fits the experimental equilibrium data better than the Freundlich model. Therefore, adsorption of this set of CECs occurs mainly at specific homogeneous sites on the adsorbent surface and, once a molecule occupies a site, no further adsorption can occur at that site, thereby forming a monolayer (Halsey, 1952). Thus, maximal adsorption (q_{max}) calculated by the Langmuir model was used for the evaluation of adsorption efficiency (Fig. 3).

For all CECs studied, adsorption onto activated peach stone biochar was 2–10 times lower than onto activated straw and softwood biochar (1.1–9.2 mg g^{-1} versus 4.3–22.8 mg g^{-1}; Figs. 2 and 3). According to the q_{max} data, the highest uptake was observed for triclosan and bisphenol A onto activated softwood biochar. However, adsorption of all CECs was lower on activated PS biochar, which had high microporosity and lower amounts of mesopores and transport macropores (external surface area 67.2–48.4 $m^2\ g^{-1}$), compared to SWP activated biochar (external surface area 164.4–152.2 $m^2\ g^{-1}$) and WSP activated biochar (external surface area 93.2–89.5 $m^2\ g^{-1}$). These results are in good agreement with previous findings showing the importance of mesoporosity for the ability of activated biochars to adsorb organic substances (Yao et al., 2020).

The presence of mesopores facilitates availability of pore surfaces for organic molecules, resulting in higher adsorption rates (Piai et al., 2019). Adsorption of caffeine and chloramphenicol, the most hydrophilic substances of the six compounds observed, was high onto activated WSP biochar. This may be explained by incomplete removal of residual ash from WSP activated biochar by the acid wash (Table 2). The inorganic matter that forms ash is more hydrophilic than the biochar carbon skeleton. More hydrophilic inorganic domains of biochar have more polar functional groups and may have greater affinity towards hydrophilic compounds (Tan et al., 2015). However, the impact of ash-forming elements in different types of biomass on CEC adsorption may vary from complete to no removal, depending on the biomass composition and on the hydrophilic-hydrophobic properties of the CECs (Guérin et al., 2020).

Pyrolysis and activation of the feedstocks used in this study generated biochar materials with varying porosity and CEC adsorption capability, possibly due to differences in biomass composition. Previous studies (Park et al., 2013; Tan et al., 2017) showed that feedstock composition (e.g., lignin, cellulose, hemicellulose) and inorganics (ash) might influence the carbonization process and the properties (i.e., porosity, surface functionality, elemental composition and ash content) of chemically activated biochar. Cellulose and lignin are the main components contributing to surface area development during chemical activation by KOH, since they are more stable than hemicellulose (Rodriguez Correa et al., 2017). Therefore, feedstock composition could also be expected to influence the adsorption properties of CO_2-activated biochar, as suggested by this study. For instance, adsorption of all CECs was low on activated biochar produced from peach stones, the feedstock with the highest lignin content. Further research is necessary to enable reliable prediction of adsorption performance of activated biochar based on feedstock composition.

Many published adsorption studies focus on the removal of single components from water, despite the facts that wastewater and natural water usually contain numerous contaminants and that the adsorption behaviour of a multi-contaminant mixture will differ from that of a single-component system (Mansouri et al., 2015). Caffeine adsorption from a single component solution performed in our other study (Wurzer & Mašek, 2021) with comparable biochar was much greater than removal from a multicomponent solution, i.e., 42 mg g^{-1} versus 22.8

Table 3
Adsorption properties of activated biochars and activated carbon Norit GSX.

Substance	Material	Models of adsorption					
		Langmuir			Freundlich		
		q_{sat}, mg g^{-1}	K_L, L g^{-1}	R^2	K_F, L mg^{-1}	n	R^2
Caffeine	WSP550A	22.8	1.1	0.95	12.4	5.9	0.94
	WSP700A	22.2	0.7	0.91	12.1	6.4	0.94
	SWP500A	11.3	6.7	0.80	10.0	28.3	0.86
	SWP700A	11.6	0.1	0.91	2.5	3.3	0.72
	PS550A	1.8	0.2	0.95	0.6	4.2	0.96
	PS700A	1.6	0.1	0.96	0.4	3.3	0.90
	AC Norit GSX	42.4	18.8	0.93	33.7	12.9	0.94
Chloramphenicol	WSP550A	11.3	1.6	0.89	8.0	10.6	0.95
	WSP700A	10.0	1.4	0.93	7.9	17.5	0.72
	SWP500A	8.8	0.3	0.96	4.6	6.9	0.79
	SWP700A	6.4	0.3	0.83	3.5	7.3	0.76
	PS550A	1.6	0.2	0.89	0.6	4.3	0.74
	PS700A	1.1	0.1	0.81	0.2	2.6	0.81
	AC Norit GSX	36.5	35.2	0.87	32.8	31.2	0.83
Carbamazepine	WSP550A	15.9	1.3	0.89	10.1	7.9	0.82
	WSP700A	16.1	1.4	0.88	10.2	7.9	0.78
	SWP500A	20.5	0.3	0.86	11.7	7.9	0.97
	SWP700A	15.4	0.4	0.76	8.3	6.8	0.90
	PS550A	3.6	0.1	0.97	0.3	2.0	0.90
	PS700A	1.5	0.1	0.94	0.5	4.0	0.80
	AC Norit GSX	53.7	1.4	0.97	38.1	10.8	0.95
Bisphenol A	WSP550A	17.5	0.9	0.94	12.4	12.0	0.75
	WSP700A	14.2	1.3	0.71	12.0	27.0	0.65
	SWP500A	31.6	1.0	0.87	22.9	14.4	0.94
	SWP700A	22.5	1.3	0.85	18.5	17.8	0.97
	PS550A	6.3	0.1	0.98	2.1	4.5	0.75
	PS700A	6.0	0.1	0.93	1.6	3.7	0.81
	AC Norit GSX	57.9	2.7	0.94	42.4	10.0	0.95
Diclofenac	WSP550A	6.7	1.2	0.79	5.2	16.3	0.68
	WSP700A	6.1	0.1	0.93	1.3	3.15	0.80
	SWP500A	5.5	0.1	0.90	1.4	3.7	0.73
	SWP700A	4.3	0.1	0.94	1.2	3.7	0.91
	PS550A	1.4	0.2	0.90	0.4	3.7	0.90
	PS700A	1.2	0.1	0.86	0.4	4.2	0.67
	AC Norit GSX	28.3	1.6	0.97	22.0	15.6	0.89
Triclosan	WSP550A	20.3	2.0	0.95	16.1	15.2	0.80
	WSP700A	18.6	2.3	0.93	16.1	29.0	0.83
	SWP500A	30.2	2.4	0.85	21.8	9.3	0.96
	SWP700A	26.5	2.0	0.93	18.0	7.9	0.95
	PS550A	9.2	0.7	0.83	5.7	7.7	0.72
	PS700A	8.4	1.0	0.82	5.5	8.2	0.78
	AC Norit GSX	75.9	1.4	0.94	48.9	7.1	0.95

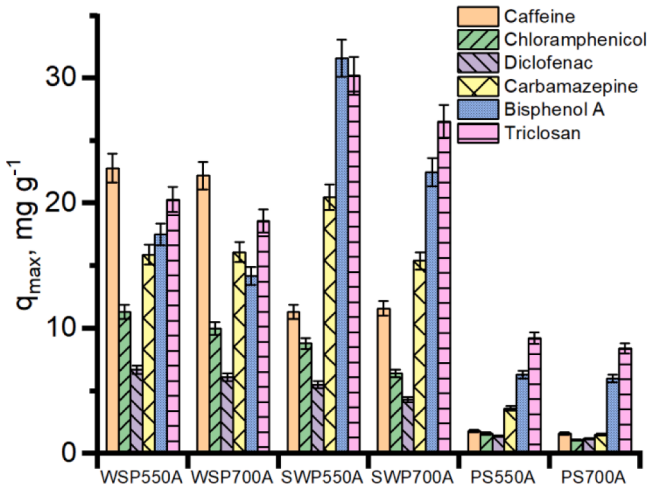

Fig. 3. Maximal adsorption (q_{max}) for caffeine, chloramphenicol, carbamazepine, bisphenol A, diclofenac, and triclosan on activated biochar from wheat straw (WSP550A and WSP700A), softwood (SWP550A and SWP700A), and peach stones (PS550A and PS700A).

mg g^{-1} on WSP, and 135 mg g^{-1} versus 11.3 mg g^{-1} on SWP.

Mansouri et al. (2015) showed that, due to competitive adsorption onto AC, the uptake of ibuprofen and amoxicillin from a binary solution was lower than uptake of the same substances from single-component solutions. The main competitive effects could be associated with the affinity of the individual compounds to the carbon adsorbent (Mansouri et al., 2015). The AC surface was considered non-polar, which contributes to the adsorption of non-polar substances rather than polar substances (Wu et al., 2020). The emerging hypothesis was, therefore, that hydrophobicity is an important parameter for CEC adsorption onto porous carbon materials. Hence, it would be logical to assume that adsorption would co-vary with K_{ow}, one of the selection criteria for CECs observed in this study.

However, covariation with K_{ow} was not observed (Fig. 3). For example, the removal of diclofenac (K_{ow} = 4.06) was more similar to that of caffeine and chloramphenicol, both hydrophilic substances, than to the hydrophobic bisphenol A and triclosan. This observation is explained by the ionised form of diclofenac in aqueous solutions at neutral pH, which renders its properties more hydrophilic than hydrophobic. The distribution coefficient (log *D*) would, therefore, be a more appropriate descriptor of ionisable compounds like diclofenac which may exist in various different ionic forms at a given pH, and is used instead of K_{ow} for further discussion. This observation has another

consequence. Adsorption of ionic or zwitterionic CECs is pH-dependent. For instance, the adsorption of acetaminophen, cephalexin and valsartan was approximately 10–70 % higher at pH 3 than at pH 10 on biochar obtained from oil palm fiber (Grisales-Cifuentes et al., 2021).

The distribution coefficient, typically expressed in logarithmic form log D, is a measure of pH-dependent differential solubility in an octanol/water system at a particular pH (Li et al., 2018a). Adsorption of more hydrophobic substances, i.e., with a distribution coefficient $>$ 3.0 (bisphenol A (log D = 3.63) and triclosan (log D = 5.13)), from the multicomponent solution studied was greatest onto SWP550A biochar (31.6 and 30.2 mg g^{-1}, respectively). The SWP550A biochar also had the highest specific (530.3 m^2 g^{-1}) and external (164.4 m^2 g^{-1}) surface area of all the biochar materials studied (Fig. 3).

Overall, pyrolysis and activation of the feedstocks used in this study generated biochar with varying porosity and CEC adsorption capability, possibly due to differences in feedstock composition (e.g., lignin, cellulose, hemicellulose) and inorganics (ash). The activated biochar obtained from three lignocellulosic feedstocks exhibited varying capabilities for removing CECs from a multicomponent water solution. Structural parameters related to porosity and ash content of the activated biochar and hydrophobic properties of the CECs were found to influence biochar adsorption efficiency. Activation increased porosity development of the biochar to over 400 m^2 g^{-1}, compared to 15.9 – 316 m^2 g^{-1} in biochar after pyrolysis. Activation of straw and softwood biochar led to development of more mesoporous ACs whereas activated peach stone biochar contained mainly micropores. Hence adsorption of all CECs was 2–10 times lower onto activated biochar from peach stones than onto activated biochar from the other materials.

The presence of mesopores can facilitate availability of porous space of carbon materials for organic molecules, resulting in higher adsorption rates. Adsorption of more hydrophobic substances (i.e., bisphenol A and triclosan) was highest (31.6 and

30.2 mg g^{-1}) onto activated biochar from softwood, the material with the highest specific (530.3 m^2 g^{-1}) and external (164.4 m^2 g^{-1}) surface area. Adsorption of caffeine and chloramphenicol, the most hydrophilic substances of those evaluated, was high onto wheat straw activated biochar with high ash content.

4. Conclusions

This study showed that the lignocellulosic biomass composition had an effect on the microstructure of the biochar and, subsequently, on their CECs removal performance. Further research should, therefore, focus on systematic studies of effects of lignocellulosic biomass components, pyrolysis, and activation conditions (temperature, time, activating agents) on the structural and adsorption properties of activated biochar. Multicomponent adsorption of CECs at environmentally relevant concentrations and impact of water matrix also warrants further study. Resulting information will be essential for the selection and eventual pre-treatment of lignocellulosic feedstocks, and for the optimization of processing conditions for activated biochar intended for environmental applications.

CRediT authorship contribution statement

Ivan Kozyatnyk: Conceptualization, Funding acquisition, Methodology, Investigation, Visualization, Writing – original draft. **Pierre Oesterle:** Methodology, Investigation, Writing – original draft. **Christian Wurzer:** Methodology, Investigation, Writing – original draft. **Ondřej Mašek:** Funding acquisition, Supervision, Conceptualization, Writing - review & editing. **Stina Jansson:** Funding acquisition, Supervision, Conceptualization, Writing - review & editing.

Declaration of Competing Interest

The authors declare that they have no known competing financial interests or personal relationships that could have appeared to influence the work reported in this paper.

Acknowledgement

The authors gratefully acknowledge Bio4Energy, a strategic research environment appointed by the Swedish government, for supporting this work. The Kempe Foundation is gratefully acknowledged for a post-doctoral fellowship for Ivan Kozyatnyk [grant number SMK-1552]. This work was supported by a STSM Grant from COST Action FP1306 [grant number 39430] and from the European Union's Horizon 2020 research and innovation programme under the Marie Skłodowska-Curie [grant number 721991].

Appendix A. Supplementary data

Supplementary data to this article can be found online at https://doi.org/10.1016/j.biortech.2021.125561.

References

Abdel daiem, M.M., Rivera-Utrilla, J., Sánchez-Polo, M., Ocampo-Pérez, R., 2015. Single, competitive, and dynamic adsorption on activated carbon of compounds used as plasticizers and herbicides. Sci. Total Environ. 537, 335–342.

Ahmed, M.B., Zhou, J.L., Ngo, H.H., Guo, W., Chen, M., 2016. Progress in the preparation and application of modified biochar for improved contaminant removal from water and wastewater. Bioresour. Technol. 214, 836–851.

Bayer, P., Heuer, E., Karl, U., Finkel, M., 2005. Economical and ecological comparison of granular activated carbon (GAC) adsorber refill strategies. Water Res. 39 (9), 1719–1728.

Bernal, V., Giraldo, L., Moreno-Piraján, J.C., 2018. Physicochemical properties of activated carbon: their effect on the adsorption of pharmaceutical compounds and adsorbate–adsorbent interactions. C—J. Carbon Res. 4 (4), 62.

Blasi, C.D., Galgano, A., Branca, C., 2019. Exothermic events of nut shell and fruit stone pyrolysis. ACS Sustain. Chem. Eng. 7 (9), 9035–9049.

Buerge, I.J., Poiger, T., Müller, M.D., Buser, H.-R., 2003. Caffeine, an anthropogenic marker for wastewater contamination of surface waters. Environ. Sci. Technol. 37 (4), 691–700.

Cagnon, B., Py, X., Guillot, A., Stoeckli, F., Chambat, G., 2009. Contributions of hemicellulose, cellulose and lignin to the mass and the porous properties of chars and steam activated carbons from various lignocellulosic precursors. Bioresour. Technol. 100 (1), 292–298.

Dalai, A.K., Azargohar, R., 2007. Production of activated carbon from biochar using chemical and physical activation: mechanism and modeling. In: Materials, Chemicals, and Energy from Forest Biomass, Vol. 954. American Chemical Society, pp. 463–476.

Delle Site, A., 2001. Factors affecting sorption of organic compounds in natural sorbent/water systems and sorption coefficients for selected pollutants. a review. J. Phys. Chem. Ref. Data 30 (1), 187–439.

Ebele, A.J., Abou-Elwafa Abdallah, M., Harrad, S., 2017. Pharmaceuticals and personal care products (PPCPs) in the freshwater aquatic environment. Emerg. Contam. 3 (1), 1–16.

Elzerman, A.W., Coates, J.T. 1987. Hydrophobic organic compounds on sediments: equilibria and kinetics of sorption. in: Sources and Fates of Aquatic Pollutants, Vol. 216, American Chemical Society, pp. 263-317.

Freundlich, H., 1907. Über die Adsorption in Lösungen. in. Zeitschrift für Physikalische Chemie 57U, 385.

Galindo-Miranda, J.M., Guízar-González, C., Becerril-Bravo, E.J., Moeller-Chávez, G., León-Becerril, E., Vallejo-Rodríguez, R., 2019. Occurrence of emerging contaminants in environmental surface waters and their analytical methodology – a review. Water Supply 19 (7), 1871–1884.

Giles, C.H., MacEwan, T.H., Nakhwa, S.N., Smith, D., 1960. 786. Studies in adsorption. Part XI. A system of classification of solution adsorption isotherms, and its use in diagnosis of adsorption mechanisms and in measurement of specific surface areas of solids. J. Chem. Soc. 3973. https://doi.org/10.1039/jr9600003973.

Grisales-Cifuentes, C.M., Serna Galvis, E.A., Porras, J., Flórez, E., Torres-Palma, R.A., Acelas, N., 2021. Kinetics, isotherms, effect of structure, and computational analysis during the removal of three representative pharmaceuticals from water by adsorption using a biochar obtained from oil palm fiber. Bioresour. Technol. 326, 124753. https://doi.org/10.1016/j.biortech.2021.124753.

Guérin, T., Ghinet, A., Hossart, M., Waterlot, C., 2020. Wheat and ryegrass biomass ashes as effective sorbents for metallic and organic pollutants from contaminated water in lab-engineered cartridge filtration system. Bioresour. Technol. 318, 124044. https://doi.org/10.1016/j.biortech.2020.124044.

Halsey, G.D., 1952. The role of surface heterogeneity in adsorption. In: Frankenburg, W. G., Komarewsky, V.I., Rideal, E.K. (Eds.), Advances in Catalysis, Vol. 4. Academic Press, pp. 259–269.

Kozyatnyk, I., Yacout, D.M.M., Van Caneghem, J.o., Jansson, S., 2020. Comparative environmental assessment of end-of-life carbonaceous water treatment adsorbents. Bioresour. Technol. 302, 122866. https://doi.org/10.1016/j.biortech.2020.122866.

Langmuir, I., 1918. The adsorption of gases on plane surfaces of glass, mica and platinum. J. Am. Chem. Soc. 40 (9), 1361–1403.
Li, H., Cao, Y., Zhang, D.i., Pan, B.o., 2018a. pH-dependent K_{OW} provides new insights in understanding the adsorption mechanism of ionizable organic chemicals on carbonaceous materials. Sci. Total Environ. 618, 269–275.
Li, W., Amos, K., Li, M., Pu, Y., Debolt, S., Ragauskas, A.J., Shi, J., 2018b. Fractionation and characterization of lignin streams from unique high-lignin content endocarp feedstocks. Biotechnol. Biofuels. 11(1), 304.
Mailler, R., Gasperi, J., Coquet, Y., Buleté, A., Vulliet, E., Deshayes, S., Zedek, S., Mirande-Bret, C., Eudes, V., Bressy, A., Caupos, E., Moilleron, R., Chebbo, G., Rocher, V., 2016. Removal of a wide range of emerging pollutants from wastewater treatment plant discharges by micro-grain activated carbon in fluidized bed as tertiary treatment at large pilot scale. Sci. Total Environ. 542 (Pt A), 983–996.
Mansouri, H., Carmona, R.J., Gomis-Berenguer, A., Souissi-Najar, S., Ouederni, A., Ania, C.O., 2015. Competitive adsorption of ibuprofen and amoxicillin mixtures from aqueous solution on activated carbons. J. Colloid Interface Sci. 449, 252–260.
Mašek, O., Buss, W., Roy-Poirier, A., Lowe, W., Peters, C., Brownsort, P., Mignard, D., Pritchard, C., Sohi, S., 2018. Consistency of biochar properties over time and production scales: a characterisation of standard materials. J. Anal. Appl. Pyrolysis 132, 200–210.
Mohan, D., Sarswat, A., Ok, Y.S., Pittman, C.U., 2014. Organic and inorganic contaminants removal from water with biochar, a renewable, low cost and sustainable adsorbent – a critical review. Bioresour. Technol. 160, 191–202.
Mustafa, M., Kozyatnyk, I., Gallampois, C., Oesterle, P., Östman, M., Tysklind, M., 2021. Regeneration of saturated activated carbon by electro-peroxone and ozonation: Fate of micropollutants and their transformation products. Sci. Total Environ. 776, 145723. https://doi.org/10.1016/j.scitotenv.2021.145723.
Park, J., Hung, I., Gan, Z., Rojas, O.J., Lim, K.H., Park, S., 2013. Activated carbon from biochar: Influence of its physicochemical properties on the sorption characteristics of phenanthrene. Bioresour. Technol. 149, 383–389.
Patel, M., Kumar, R., Kishor, K., Mlsna, T., Pittman, C.U., Mohan, D., 2019. Pharmaceuticals of emerging concern in aquatic systems: chemistry, occurrence, effects, and removal methods. Chem. Rev. 119 (6), 3510–3673.
Piai, L., Dykstra, J.E., Adishakti, M.G., Blokland, M., Langenhoff, A.A.M., van der Wal, A., 2019. Diffusion of hydrophilic organic micropollutants in granular activated carbon with different pore sizes. Water Res. 162, 518–527.
Rizzo, L., Malato, S., Antakyali, D., Beretsou, V.G., Đolić, M.B., Gernjak, W., Heath, E., Ivancev-Tumbas, I., Karaolia, P., Lado Ribeiro, A.R., Mascolo, G., McArdell, C.S., Schaar, H., Silva, A.M.T., Fatta-Kassinos, D., 2019. Consolidated vs new advanced treatment methods for the removal of contaminants of emerging concern from urban wastewater. Sci. Total Environ. 655, 986–1008.
Rodriguez Correa, C., Otto, T., Kruse, A., 2017. Influence of the biomass components on the pore formation of activated carbon. Biomass Bioenergy 97, 53–64.
Sajjadi, B., Chen, W.-Y., Egiebor Nosa, O., 2019. A comprehensive review on physical activation of biochar for energy and environmental applications. Rev. Chem. Eng. 35 (6), 735–776.
Schimmelpfennig, S., Glaser, B., 2012. One step forward toward characterization: some important material properties to distinguish biochars. J. Environ. Qual. 41 (4), 1001–1013.
Sepúlveda-Cervantes, C.V., Soto-Regalado, E., Rivas-García, P., Loredo-Cancino, M., Cerino-Córdova, F.dJ., García Reyes, R.B., 2018. Technical-environmental optimisation of the activated carbon production of an agroindustrial waste by means response surface and life cycle assessment. Waste Manag. Res. 36 (2), 121–130.
Singh, B., Camps-Arbestain, M., Lehmann, J., 2017. Biochar: a guide to analytical methods. Csiro Publishing.
Suliman, W., Harsh, J.B., Abu-Lail, N.I., Fortuna, A.-M., Dallmeyer, I., Garcia-Perez, M., 2016. Influence of feedstock source and pyrolysis temperature on biochar bulk and surface properties. Biomass Bioenergy 84, 37–48.
Suzuki, T., Nakagawa, Y., Takano, I., Yaguchi, K., Yasuda, K., 2004. Environmental fate of bisphenol a and its biological metabolites in river water and their xeno-estrogenic activity. Environ. Sci. Technol. 38 (8), 2389–2396.
Tan, X.-F., Liu, S.-b., Liu, Y.-G., Gu, Y.-L., Zeng, G.-M., Hu, X.-J., Wang, X., Liu, S.-H., Jiang, L.-H., 2017. Biochar as potential sustainable precursors for activated carbon production: Multiple applications in environmental protection and energy storage. Bioresour. Technol. 227, 359–372.
Tan, X., Liu, Y., Zeng, G., Wang, X., Hu, X., Gu, Y., Yang, Z., 2015. Application of biochar for the removal of pollutants from aqueous solutions. Chemosphere 125, 70–85.
Thommes, M., Kaneko, K., Neimark, A.V., Olivier, J.P., Rodriguez-Reinoso, F., Rouquerol, J., Sing, K.S.W., 2015. Physisorption of gases, with special reference to the evaluation of surface area and pore size distribution (IUPAC Technical Report). Pure Appl. Chem. 87 (9–10), 1051–1069.
Thompson, K.A., Shimabuku, K.K., Kearns, J.P., Knappe, D.R.U., Summers, R.S., Cook, S. M., 2016. Environmental comparison of biochar and activated carbon for tertiary wastewater treatment. Environ. Sci. Technol. 50 (20), 11253–11262.
Wang, L., Ok, Y.S., Tsang, D.C.W., Alessi, D.S., Rinklebe, J., Wang, H., Mašek, O., Hou, R., O'Connor, D., Hou, D., Nicholson, F., 2020. New trends in biochar pyrolysis and modification strategies: feedstock, pyrolysis conditions, sustainability concerns and implications for soil amendment. Soil Use Manag. 36 (3), 358–386.
Wu, Z., Sun, Z., Liu, P., Li, Q., Yang, R., Yang, X., 2020. Competitive adsorption of naphthalene and phenanthrene on walnut shell based activated carbon and the verification via theoretical calculation. RSC Adv. 10 (18), 10703–10714.
Wurzer, C., Mašek, O., 2021. Feedstock doping using iron rich waste increases the pyrolysis gas yield and adsorption performance of magnetic biochar for emerging contaminants. Bioresour. Technol. 321, 124473. https://doi.org/10.1016/j.biortech.2020.124473.
Yang, H., Yan, R., Chen, H., Lee, D.H., Zheng, C., 2007. Characteristics of hemicellulose, cellulose and lignin pyrolysis. Fuel 86 (12-13), 1781–1788.
Yao, X., Ji, L., Guo, J., Ge, S., Lu, W., Chen, Y., Cai, L.u., Wang, Y., Song, W., 2020. An abundant porous biochar material derived from wakame (Undaria pinnatifida) with high adsorption performance for three organic dyes. Bioresour. Technol. 318, 124082. https://doi.org/10.1016/j.biortech.2020.124082.
Yunus, Z.M., Al-Gheethi, A., Othman, N., Hamdan, R., Ruslan, N.N., 2020. Removal of heavy metals from mining effluents in tile and electroplating industries using honeydew peel activated carbon: a microstructure and techno-economic analysis. J. Clean. Prod. 251, 119738. https://doi.org/10.1016/j.jclepro.2019.119738.
Zhao, L., Cao, X., Mašek, O., Zimmerman, A., 2013. Heterogeneity of biochar properties as a function of feedstock sources and production temperatures. J. Hazard. Mater. 256-257, 1–9.
Zhu, X., Li, C., Li, J., Xie, B., Lü, J., Li, Y., 2018. Thermal treatment of biochar in the air/nitrogen atmosphere for developed mesoporosity and enhanced adsorption to tetracycline. Bioresour. Technol. 263, 475–482.